Differential regulation of the Wilms' tumor gene, WT1, during differentiation of embryonal carcinoma and embryonic stem cells.

Document status and date:
Published: 01/01/1997

Document Version:
Publisher's PDF, also known as Version of Record (includes final page, issue and volume numbers)

Please check the document version of this publication:

• A submitted manuscript is the version of the article upon submission and before peer-review. There can be important differences between the submitted version and the official published version of record. People interested in the research are advised to contact the author for the final version of the publication, or visit the DOI to the publisher's website.
• The final author version and the galley proof are versions of the publication after peer review.
• The final published version features the final layout of the paper including the volume, issue and page numbers.
Link to publication

Download date: 04. Oct. 2023

Differential Regulation of the Wilms' Tumor Gene, *WT1*, during Differentiation of Embryonal Carcinoma and Embryonic Stem Cells[1]

Volkher Scharnhorst, Onno Kranenburg,[2] Alex J. van der Eb, and Aart G. Jochemsen[3]

Laboratory of Molecular Carcinogenesis, Sylvius Laboratories, Leiden University, P. O. Box 9503, 2300 RA Leiden, the Netherlands

Abstract

The expression pattern of the Wilms' tumor suppressor gene, *WT1*, during embryonal development suggests a role for the WT1 proteins in the differentiation of specific tissues. This notion is supported by the observation that *WT1* knock-out mice fail to develop kidneys and gonads. We describe here the changes in the expression and DNA binding activity of the *WT1* gene product in P19 embryonal carcinoma cells and embryonic stem cells triggered to differentiate by either retinoic acid (RA) or DMSO.

In exponentially growing P19 embryonal carcinoma (EC) cells, *WT1* mRNA and proteins were undetectable. During RA-induced but not DMSO-induced differentiation of P19 EC cells, WT1 expression and DNA binding are strongly activated. Treatment of embryonic stem cells with RA resulted in a similar activation of WT1. Immunohistochemical analysis showed that WT1 is expressed in endodermal, glial, and epithelial cell types.

In addition, DNA binding by EGR-1, a transcription factor structurally related to WT1, increased during differentiation of P19 EC and embryonic stem cells. To investigate the possible functional consequences of DNA binding by WT1, we examined the expression levels of two putative transcriptional targets of WT1, the insulin-like growth factor I receptor and epidermal growth factor receptor. We found that after an initial induction, decreasing expression of the insulin-like growth factor I receptor is correlated with increasing WT1 expression.

Our results demonstrate that expression of WT1 is induced in specific cell types during RA-induced differentiation of P19 EC cells, reflecting the tissue-specific expression of WT1 *in vivo*. Therefore, we believe that P19 EC cells are a suitable system to study activation and function of WT1 during differentiation.

Introduction

Wilms' tumor is a pediatric kidney neoplasm that affects 1 in 10,000 children and is thought to arise from multipotent renal stem cells that fail to differentiate properly (1). The Wilms' tumor 1 gene, *WT1*,[4] is one of at least three genes believed to be involved in the development of this tumor. WT1 (reviewed in Ref. 2) is expressed primarily in the condensing mesenchyme, the renal vesicles, and the glomerular epithelium of the developing kidney (3, 4) and is homozygously mutated or deleted in a subset of Wilms' tumors. Furthermore, certain heterozygous mutations or deletions in the *WT1* gene give rise to congenital anomalies that are found in the Denys-Drash and the WAGR (Wilms' tumor, aniridia, genitourinary abnormalities, mental retardation) syndrome, respectively (reviewed in Refs. 5 and 6). These findings suggest that WT1 plays an important role during the development of the urogenital system. This notion is strongly supported by the observation that mice lacking WT1 expression fail to develop kidney and gonads (7) and die during embryogenesis. Apart from the developing epithelia of the kidneys, testes, and ovaries, WT1 expression is detected in the mesothelium, the stromal component of the spleen, and certain areas of the central nervous system (5, 6). Investigations on the regulation and function of WT1 during differentiation have been hampered by the limited availability of pluripotent cell lines that express this gene at detectable levels. *WT1* mRNA levels were found to be down-regulated at the posttranscriptional level during erythroid/megakaryocytic differentiation of K562 erythroleukemia cells and myelomonocytic differentiation of HL60 promyeloid leukemia cells (8, 9). Kinane *et al.* (10, 11) demonstrated that EGR-1 levels are down-regulated and WT1 levels are up-regulated in the polarizing LLC-PK1 pig kidney cell line, which is paralleled by binding of WT1 to the EGR-1 DNA consensus sequence (10, 11). Until now, most other studies on WT1 have been performed under nonphysiological conditions in cell lines that ectopically express WT1.

Therefore, we investigated the regulation of WT1 in pluripotent P19 EC cells that originate from an ES cell-induced tumor (12) and are frequently used to study the molecular mechanisms underlying early developmental processes. ES cells (13–15) and P19 EC cells (16) can be triggered to differentiate into a variety of cell types. Treatment of P19 EC cells with RA induces formation of endodermal and (neuro)-ectodermal cells, including neurons and glial cells (17–19),

whereas DMSO-induced differentiation leads to mesodermal and endodermal derivatives (19–21). End-2, Epi-7 (22), and Mes-1 (23) cells are stably differentiated clonal cell lines derived from P19 EC cells differentiated by RA and DMSO, respectively. These cell lines have been characterized as visceral-endoderm like (End-2), epithelial (Epi-7), and meso-dermal (Mes-1) by morphology, expression of marker proteins, and response to growth factors (22, 23).

The *WT1* gene encodes a zinc-finger protein of the Cys_2-His_2 type with homology to the EGR-1 protein family of transcription factors (reviewed in Ref. 24). Four *WT1* mRNAs resulting from two alternative splicing events have been identified (25). Alternative splice I results in the inclusion or exclusion of exon 5, which encodes 17 amino acids just NH_2-terminal to the four zinc fingers. Alternative splice II involves the use of a splice acceptor site in exon 9, resulting in the presence or absence of a three-amino acid (KTS) insert between zinc fingers 3 and 4. The resulting M_r 52,000–54,000 WT1 isoforms (26) are transcription factors that, depending on promoter context and cell type, repress or activate transcription (2). WT1 modulates the promoter activity of several genes encoding growth factors or growth factor receptors such as the *platelet-derived growth factor A-chain* (27), *IGF-II* (28), *transforming growth factor β1* (29), the *IGFI-R* (30, 31), and the *EGF-R* (32) and also promoters of genes encoding transcription factors including the *PAX-2* (33) and *EGR-1* (34) promoters.

In addition to its function as a transcription factor, WT1 may also be involved in posttranscriptional processing of RNA (35, 36). The WT1 isoforms containing the three amino acid residues KTS between zinc fingers 3 and 4 do not readily bind the EGR-1 (37, 38) or a similar consensus sequence, termed WTE (38, 39), but preferentially colocalize and associate with splicing factors (35).

We show here that WT1 expression and DNA binding activity are strongly induced during RA-induced but not during DMSO-induced differentiation of P19 EC cells. In line with this, we found that in two cell lines derived from RA-triggered differentiation of P19 EC cells, End-2 and Epi-7, WT1 expression is high, whereas it is undetectable in the mesodermal Mes-1 cell line. Our results suggest that expression of WT1 during differentiation of P19 EC cells is limited to certain cell types, including endodermal, glial, and epithelial cells, resembling tissue-specific expression in the developing embryo. Because WT1 expression is distinctively modulated during differentiation of pluripotent P19 EC cells along different pathways, P19 EC cells are a suitable system to study the regulation and function of WT1 in development.

Results
Up-Regulation of the Steady-State *WT1* mRNA Level during RA-Induced Differentiation of P19 EC Cells.
Differentiation of P19 EC cells can be induced by either RA or DMSO. Treatment of aggregated P19 EC cells with RA leads to formation of endodermal and (neuro)ectodermal cell types, whereas the addition of DMSO to P19 EC cell aggregates gives rise to endoderm- and mesoderm-derived cell types, including cardiac and skeletal muscle. Treatment of P19 EC cells with RA in monolayer triggers differentiation into a less

well-defined mixture of cells, including fibroblast-like and endodermal cells (40). To determine whether *WT1* mRNA levels are differentially altered during P19 EC cell differentiation along distinct pathways, we isolated total RNA from proliferating P19 EC cells, P19 EC cells treated in monolayer with 1 μM RA for 1–6 days, and P19 EC cells that had been aggregated in the presence of either 0.5 μM RA or 1% DMSO. In addition, we isolated RNA from two clonal cell lines derived from differentiated P19 EC cells, the Epi-7 and Mes-1 cell lines. As a control, we isolated RNA from an adenovirus-transformed baby rat kidney cell line stably expressing the WT1 isoform lacking both splice inserts from a human cDNA construct (38). Northern blot analysis showed that *WT1* mRNA was undetectable in P19 EC cells. The steady-state *WT1* mRNA levels increase markedly in P19 EC cells grown in monolayer in the presence of RA. The *WT1* transcript of 3.6 kb was first detected on day 3 and increased in abundance up to day 6 of differentiation (Fig. 1*A*). P19 EC cells treated as aggregates with RA exhibited a similar induction of *WT1* mRNA, starting on day 2 after replating (data not shown). However, the mRNA levels stayed markedly lower than in P19 EC cells differentiated in monolayer. The amount of *WT1* mRNA in Epi-7 cells is approximately equal to the amount detected on day 6 of monolayer differentiation (Fig. 1*A*). *WT1* mRNA was undetectable in P19 EC cells aggregated in the presence of DMSO (data not shown) and the myoblast-like Mes-1 cell line (Fig. 1*A*). Thus, the steady-state level of *WT1* mRNA is increased during RA-induced but not during DMSO-induced P19 EC cell differentiation. At present, we cannot distinguish between the possibilities of increased mRNA stability, enhanced transcription, or a combination of both.

Differential Regulation of WT1 Protein Levels in P19 EC Cells during RA-Induced and DMSO-Induced Differentiation.
To investigate whether the induction of *WT1* mRNA leads to increased protein levels, we prepared cell lysates for 6 to 8 consecutive days of differentiation induced by 1 μM RA, 0.5 μM RA, or 1% DMSO and analyzed these by Western blotting with an anti-WT1 antibody. Lysates prepared from exponentially growing P19 EC cells do not contain detectable amounts of WT1 protein (Fig. 2*A*), whereas at day 4 of differentiation in monolayer, two protein bands (*thick arrow*) of about M_r 50,000 appeared, which continued to increase in intensity up to day 6 (Fig. 2*B*). In lysates of P19 EC cells that had been transiently transfected with expression vectors encoding the two WT1 isoforms, which either include or lack exon 5, two protein bands appeared that exactly comigrated with the induced doublet (data not shown), strongly suggesting that both the -17 and +17 amino acid isoforms of WT1 are induced by RA treatment. The doublet that runs at higher molecular weight (*thin arrow*) than the major forms may correspond to the recently described larger isoforms that result from translation initiation 204 bp upstream of the initiator AUG (41). P19 EC cells treated as aggregates with RA displayed a rise in WT1 proteins at day 3 after replating (Fig. 2*C*). However, the amount of WT1 in these cultures remains lower than in P19 EC cells differentiated by RA in monolayer. As expected from the results obtained by Northern blot analysis,
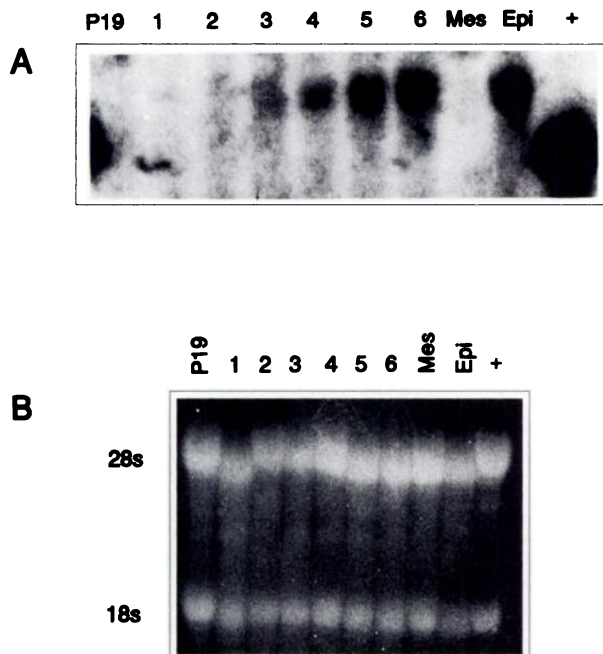
Fig. 1. Northern blot analysis of P19 EC cells, P19 EC cells treated with RA in monolayer for 1 to 6 days (*Lanes* 1–6), and Mes-1 and Epi-7 cells. *A*, *WT1* mRNA is undetectable in RNA samples of P19 EC and Mes-1 cells; steady-state levels of *WT1* mRNA increase from days 3 to 6 of differentiation in monolayer; *WT1* mRNA is present in Epi-7- and *WT1*-expressing AdBRK cells (+). *B*, ethidium bromide-stained agarose gel to demonstrate equal loading of RNA samples.

DMSO-treated P19 aggregates did not show any WT1 protein signal within 8 days after replating (Fig. 2*D*).

In line with these observations, we found that Epi-7 and End-2, two cell lines isolated from P19 EC cells treated as aggregates with RA (22), contain high levels of WT1, whereas the Mes-1 clonal cell line isolated from DMSO-treated P19 EC cell aggregates does not contain detectable amounts of WT1 protein (Fig. 2*A*). Thus, WT1 protein expression is restricted to cell types that result from RA-induced differentiation of P19 EC cells.

WT1 Proteins Are Localized in the Nucleus of Glial, Endodermal, and Epithelial Cells. To investigate the intracellular distribution of the WT1 proteins in P19 EC cells triggered to differentiate by RA, exponentially growing P19 EC cells and P19 EC cells treated with RA for 6 days in monolayer were analyzed by indirect immunofluorescence with an anti-WT1 antiserum. Exponentially growing P19 EC cells are WT1 negative (Fig. 3*A*). Detection of the embryonal stem cell-specific antigen SSEA-1 (42) on the membranes of P19 EC cells confirms the absence of spontaneous differentiation (Fig. 3*C*). In P19 EC cells treated with RA in monolayer for 6 days, an intense nuclear WT1 signal was detected in about 80% of the cells (Fig. 3*D*). At this time, all cells were negative for SSEA-1, demonstrating that the cells that do not express WT1 are not undifferentiated but constitute a subpopulation of differentiated, WT1-negative cells (Fig. 3*F*). When P19 EC cells aggregated in the presence of RA were monitored by immunofluorescence, we observed that the majority of the
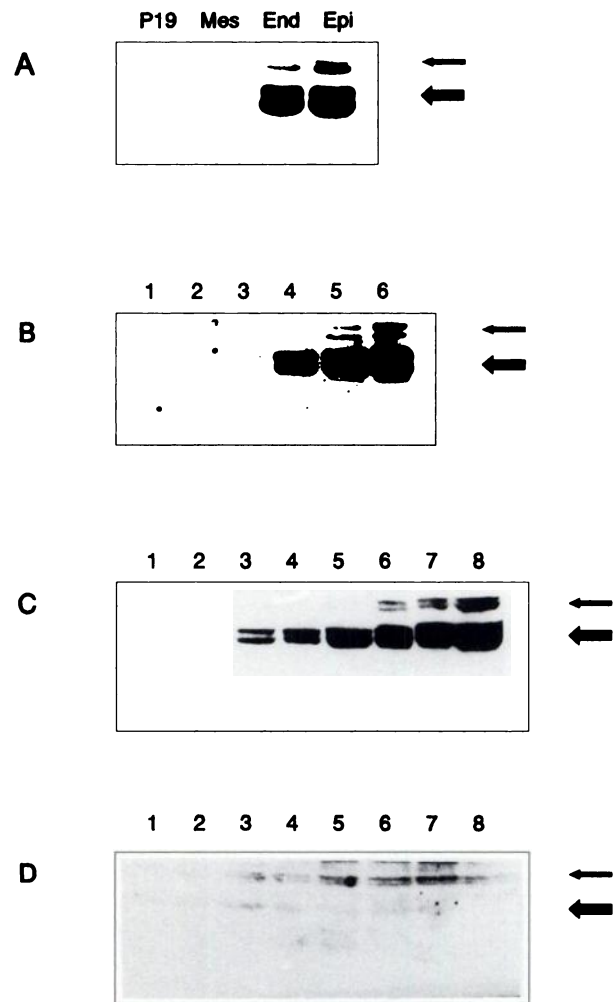
Fig. 2. Western blot analysis of WT1 protein levels in P19 EC, Mes-1, End-2, Epi-7, and differentiating P19 cells. Whole-cell lysates were separated on a 10% SDS-polyacrylamide gel and blotted. *A*, analysis of P19, Mes-1, End-2, and Epi-7 cell lysates (50 μg) showed that WT1 protein expression is restricted to End-2 and Epi-7 cells. *B*, in lysates (50 μg) of P19 cells differentiated in the presence of 1 μM RA for 1 to 6 days (*Lanes* 1–6) WT1 is first seen at day 4 and increases up to day 6 of differentiation. P19 cells aggregated for 3 days in the presence of either 0.5 μM of RA (*C*) or 1% DMSO (*D*) were replated, and lysates were prepared for 8 consecutive days (*Lanes* 1–8) after replating; 100 μg of lysate were loaded in each lane; WT1 proteins could first be detected on day 3 after replating in RA-treated aggregates (*C*), whereas WT1 is absent in P19 cells treated as aggregates with DMSO (*D*). The positions of the M_r 52,000–54,000 forms of WT1 are indicated by *thick arrows,* and the location of the larger isoforms by *thin arrows.*

cells that grow out from the replated aggregates express WT1, whereas no WT1 expression could be seen in the cells forming the aggregates (data not shown). End-2 and Epi-7 cells showed homogeneous nuclear WT1 staining, whereas DMSO-treated P19 EC as well as Mes-1 cells were WT1 negative (data not shown). To characterize the WT1-expressing cells, double immunofluorescence was performed with several immunohistochemical markers. The End-2 cell line and a subpopulation of P19 EC cells treated with RA were double-positive for WT1 and cytokeratin Endo-A (Fig. 3, *G* and *I*), indicating that a subpopu-
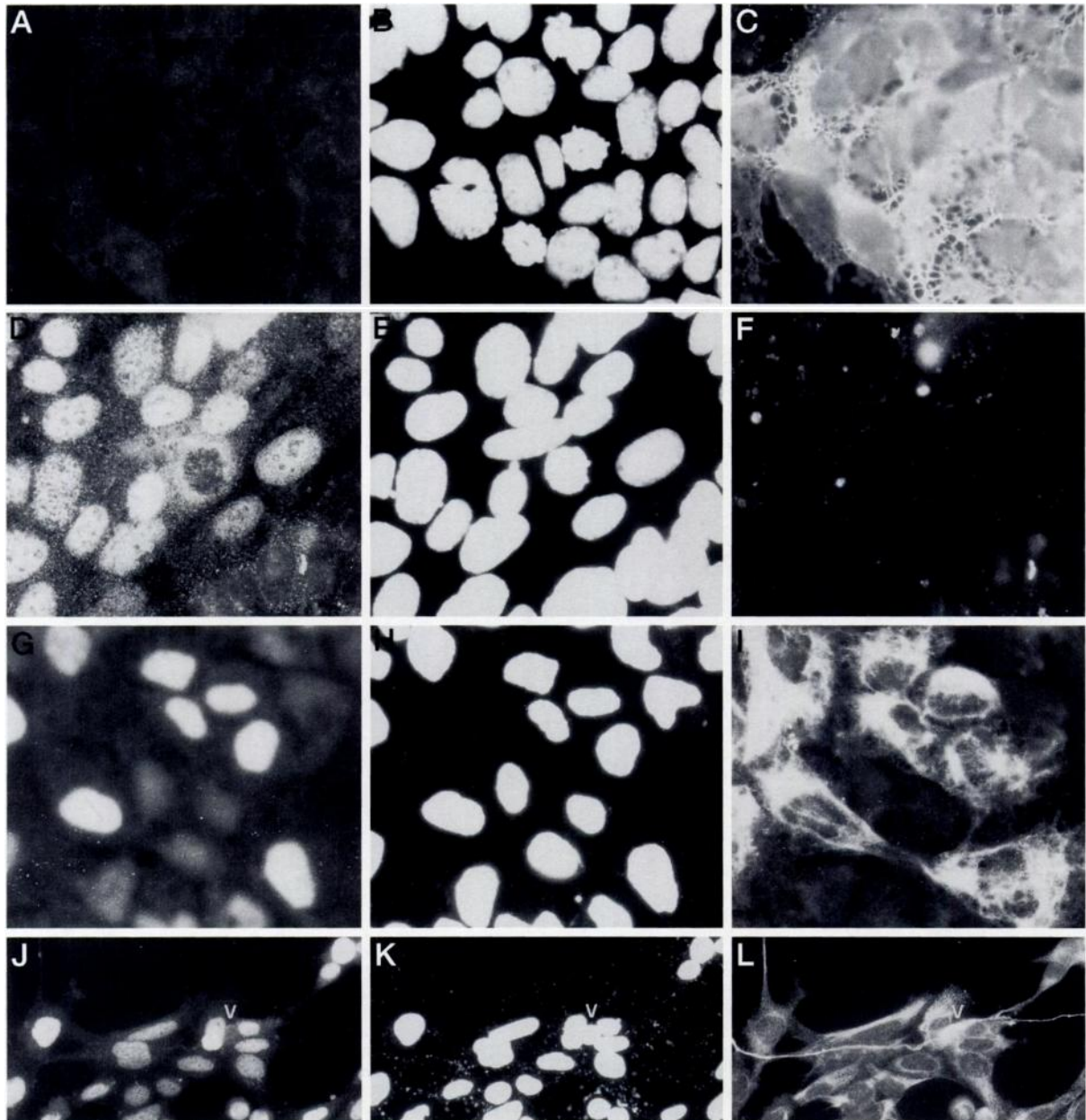
Fig. 3. Nuclear localization of WT1 proteins and coexpression of WT1 with GFAP and cytokeratin Endo-A. Cells were fixed for indirect immunofluorescence, and signals were visualized as described in "Materials and Methods." *A,* WT1 protein was undetectable in proliferating P19 cells. *B,* DAPI stain, and *C,* SSEA1 stain, of the same cells. *D,* on day 6 of differentiation triggered by 1 μM RA, the nuclei of most cells were positive for WT1. The same field stained with: *E,* DAPI, and *F,* SSEA-1, revealed that all cells are negative for SSEA1. RA-treated P19 cells coexpress WT1 (*G*) and cytokeratin Endo-A (*I*). *H,* nuclei of the same field are visualized by DAPI stain. A subpopulation of WT1-positive cells (*J*) is also positive for GFAP (*L*). *K,* DAPI stain of the same cells. The *arrowhead* marks the nucleus of a GFAP-positive, WT1-negative cell.

lation of WT1-positive cells is endodermal. However, WT1 negative cells that arise during RA- and DMSO-triggered differentiation can also express cytokeratin Endo-A (data not shown). Furthermore, several RA-treated P19 EC cells show coexpression of WT1 and GFAP, a glial cell-specific protein, but GFAP-positive cells with long processes are WT1 negative (Fig. 3, *J* and *L*). Thus, P19-derived cells, including glial, endodermal, and epithelial cells, express

WT1, and in these cells, WT1 is localized in the nucleus, as may be expected (43).

Binding of WT1 and EGR-1 Proteins to the WTE Consensus Sequence during Differentiation. WT1 and EGR-1, whose induction during RA- and DMSO-triggered differentiation of P19 EC cells as aggregates has been described previously (44), can bind to a common DNA sequence, termed WTE (38, 39). We characterized the DNA
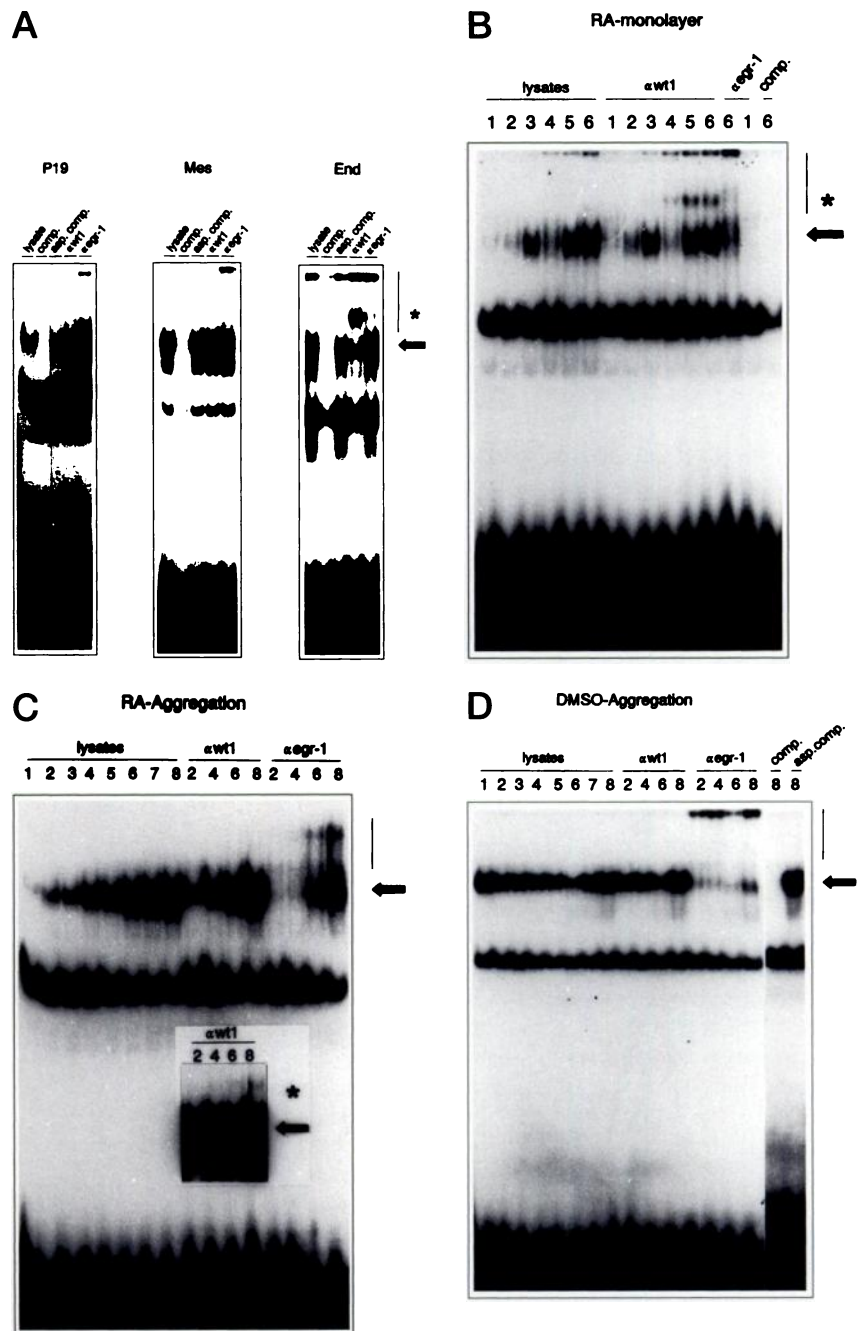
Fig. 4. Analysis of WT1 and EGR-1 DNA binding activity by electrophoretic mobility shift assay. Nuclear extracts were prepared from P19 EC, Mes-1, End-2, and differentiating P19 cells. The extracts were incubated with the ^{32}P-labeled WTE oligonucleotide alone (*lysate*), in the presence of a 100-fold excess of unlabeled WTE oligonucleotide (*comp.*), or a 100-fold excess of unlabeled aspecific competitor (*asp. comp.*), an anti-WT1 antiserum (*αwt1*), or an anti-EGR-1 antibody (*αegr-1*). *A,* in extracts of P19 and Mes-1 cells, only EGR-1 DNA binding could be detected, whereas End-2 cells contain both WT1 and EGR-1. *B,* during RA-triggered differentiation in monolayer for 1 to 6 days (*Lanes 1–6*), increasing amounts of WT1 (*αwt1*) and EGR-1 (*αegr-1*) bound to DNA could be supershifted. *C,* during 8 days after replating (*Lanes 1–8*) of P19 cells treated as aggregates with RA, little WT1 (*insert* in Fig. 4C shows a long exposure) and high amounts of EGR-1 could be supershifted (*αegr-1*). *D,* in extracts of P19 cells treated as aggregates with DMSO, only EGR-1 could be detected in the DNA-binding complex within 8 days (*Lanes 1–8*) after replating. *Arrow,* position of the specific shift; *,* position of the anti-WT1 supershift; *vertical bar,* position of the anti-EGR-1 supershift. Note that depending on the cell type, addition of the anti-EGR-1 antiserum results in a weakened specific shift, a smear above the specific shift, retention of the protein-DNA complex in the slot, or a combination of these.

binding properties of endogenous WT1 and EGR-1 to this sequence by performing electrophoretic mobility shift assays with nuclear extracts from untreated and differentiating P19 EC cells. In exponentially growing P19 EC cells, two DNA binding complexes were found (Fig. 4A, first lane from left). The upper of these complexes could be completely competed out by a 100-fold excess of unlabeled WTE oligonucleotide. The addition of anti-WT1 or anti-EGR-1 antibodies resulted in a supershift with only the anti-EGR-1 antiserum, indicating that EGR-1 is present in P19 EC cells. Nuclear lysates of P19 EC cells differentiated in monolayer showed

increased binding to the WTE oligonucleotide from day 1 up to day 6 of differentiation (Fig. 4B). A clear WT1 supershift was first detected at day 4 and increased in intensity at days 5 and 6 of differentiation. Thus, DNA binding by WT1 correlates with the induction of WT1 protein during differentiation in monolayer (Fig. 2B). When testing for the presence of EGR-1 in the complex, we found that at day 1, EGR-1 is barely detectable, but the amount is clearly increased at day 6 of monolayer differentiation.

P19 EC cells treated with RA as aggregates showed increasing binding to the WTE oligonucleotide during 8 days

after replating (Fig. 4C). Only weak supershifts could be observed following the addition of an anti-WT1 antiserum (Fig. 4C, insert), whereas the addition of an anti-EGR-1 antibody induced a strong supershift that increased in intensity up to day 8. Total binding to the WTE sequence remained constant during 8 days after replating of DMSO-treated P19 aggregates (Fig. 4D). No WT1 DNA binding could be detected, whereas the addition of an anti-EGR-1 antiserum clearly reduced the intensity of the specific complex from day 2 on, indicating that most of the DNA binding activity present in this complex is EGR-1. The DNA binding characteristics found in the End-2 and Mes-1 cell lines are analogous to those in RA- and DMSO-treated P19 EC cells, respectively (Fig. 4A). The specific DNA binding activity found in nuclear extracts of End-2 cells contains both WT1 and EGR-1, whereas only EGR-1 could be detected in extracts of the Mes-1 cell line. Mes-1 lysates contained a specific complex of lower molecular weight, which is not affected by addition of an anti-EGR-1 antibody. This band could be caused by another member of the EGR family, which binds to the WTE sequence. Both WT1 and EGR-1 were present in the DNA binding complex of Epi-7 cells (data not shown).

In summary, DNA binding by WT1 could be detected in P19 EC cells differentiated by RA and in the stable cell lines derived from RA-treated P19 EC cells, End-2 and Epi-7. EGR-1 DNA binding activity is present in all cells tested and is most prominent during differentiation of P19 EC cells in aggregates.
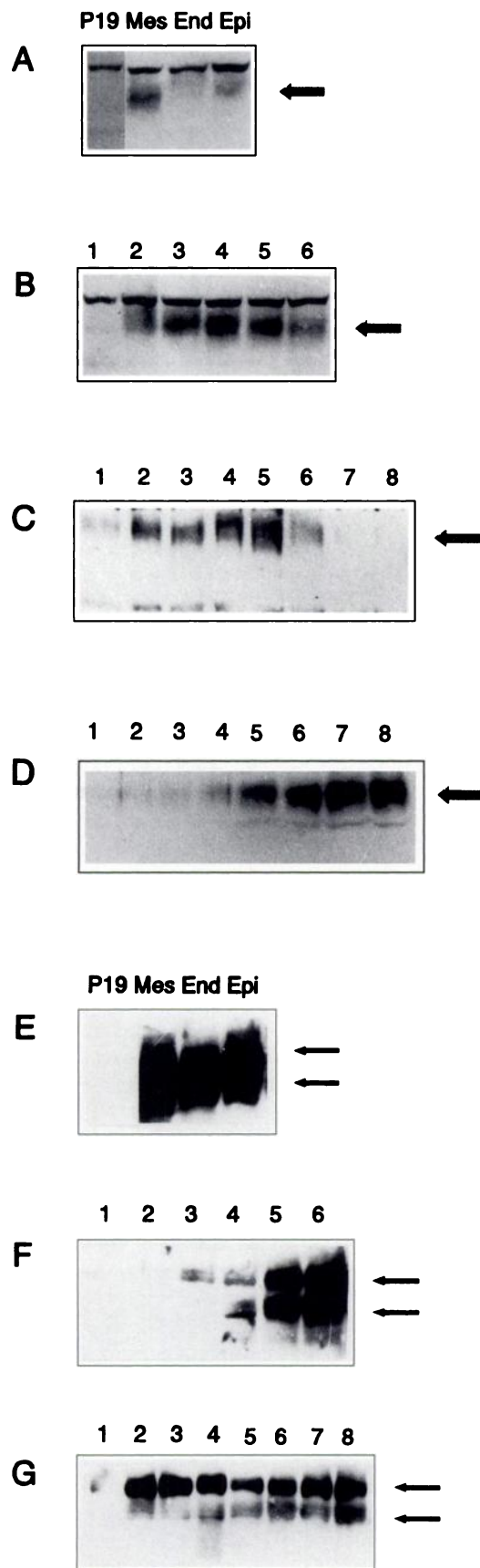
WT1 Expression and DNA Binding during RA-triggered Differentiation of ES Cells. P19 EC cells are derived from an ES cell-induced tumor (12). To investigate whether WT1 up-regulation during RA-induced differentiation of P19 EC cells is unique to EC cells or a general feature of differentiating ES cells, we investigated the effect of RA on WT1 regulation in ES cells. Fig. 5A shows increased expression of WT1 proteins in differentiating ES cells after 3 and 6 days of treatment with RA in monolayer. Similar to the situation in P19 EC cells, the WT1 proteins in ES cells are localized in the nucleus (data not shown).

Next, we studied the DNA binding properties of WT1 and EGR-1 in ES cells. Electrophoretic mobility shift analysis demonstrated that the binding pattern to the WTE sequence was analogous to the pattern in P19 EC cells (Fig. 5B). A specific complex detectable in exponentially growing ES cells could be competed out with an excess of nonradioactive WTE oligonucleotide. In this complex, only EGR-1 but no WT1 was found. Overall binding to the oligonucleotide was reduced on days 3 and 6 of differentiation, but the amount of WT1 in the DNA binding complex increased strongly. EGR-1 is present in the WTE-binding complex of proliferating ES cells; its binding diminished early after the addition of RA before rising again.

We conclude from this that in ES cells as well as in P19 EC cells, WT1 expression is induced and increasing amounts of WT1 and EGR-1 proteins bind to DNA during RA-triggered differentiation. This suggests that induction of WT1 during RA-triggered differentiation is a general phenomenon in pluripotent embryonic cells.
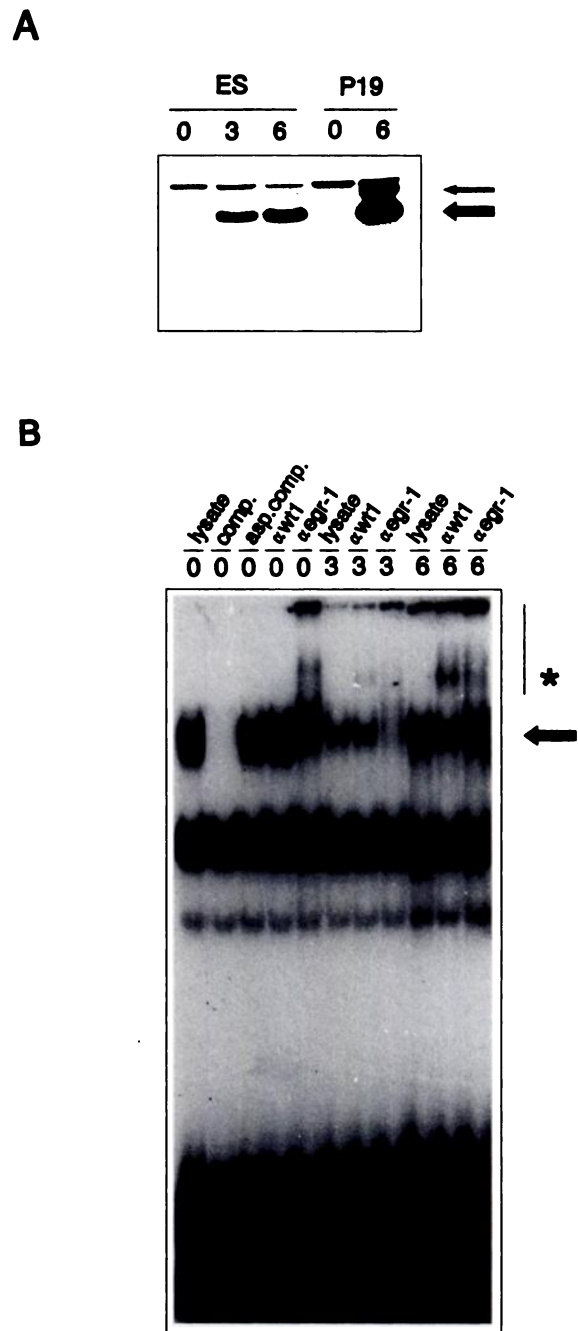
Fig. 5. WT1 expression and DNA binding patterns during RA-induced differentiation of ES cells in monolayer. *A,* Western analysis of proliferating ES cells (*Lane 0*) and ES cells treated with RA for 3 and 6 days (*Lanes 3* and *6*) revealed an increase of WT1 protein in time. As a comparison, exponentially growing P19 cells (*Lane 0*) and P19 cells differentiated for 6 days in monolayer (*Lane 6*) are shown. The positions of the M_r 52,000–54,000 forms of WT1 are indicated by a *thick arrow,* and the location of the larger isoforms by a *thin arrow. B,* electrophoretic mobility shift assay. Nuclear extracts of ES cells and ES cells treated with RA for 3 or 6 days were incubated with the labeled WTE oligo alone (*lysate*) in the presence of a 100-fold excess of unlabeled WTE (*comp.*) or aspecific competitor (*asp. comp.*); the addition of an anti-WT1 antiserum (*awt1*) revealed that WT1 is present in the DNA-binding complex of differentiating ES cells only, whereas EGR-1 is present in proliferating and differentiating ES cells (*aegr-1*). *Thick arrow,* position of the specific shift; *, position of the anti-WT1 supershift; *vertical bar,* position of the anti-EGR-1 supershift.

P19 Mes End Epi

A

1 2 3 4 5 6

B

1 2 3 4 5 6 7 8

C

1 2 3 4 5 6 7 8

D

P19 Mes End Epi

E

1 2 3 4 5 6

F

1 2 3 4 5 6 7 8

G

EGF-R and IGFI-R Levels during P19 EC Cell Differentiation. To investigate the consequences of increasing amounts of WT1 during RA-induced differentiation, we monitored the protein levels of two of its transcriptional targets, the IGFI-R and the EGF-R by Western blot analysis. IGFI-R protein was undetectable in P19 EC cells (Fig. 6A), whereas its levels were found to be elevated during differentiation of P19 EC cells (Fig. 6, B–D). RA treatment in monolayer led to an increase in IGFI-R protein until day 4, followed by a decline on days 5 and 6 (Fig. 6B). Interestingly, the decline coincides with the induction of WT1 expression. Moreover, the two WT1-expressing cell lines End-2 and Epi-7 contain a significantly lower level of IGFI-R protein than the Mes-1 cell line (Fig. 6A). Also, during differentiation of P19 EC cells treated as aggregates with RA, declining IGFI-R levels are correlated with increasing amounts of WT1 protein (Fig. 6C). DMSO-treated P19 EC cells, which do not contain WT1 proteins, showed a constant increase of IGFI-R protein up to day 8 after replating (Fig. 6D). No EGF-R protein could be detected in exponentially growing P19 EC cells (Fig. 6E). During differentiation induced by 1 μM RA a gradual increase of EGF-R was observed (Fig. 6F). In agreement with a previous publication (45), we detected a strong EGF-R signal 2 days after replating of RA-treated aggregates, which remained constant until 8 days after replating (Fig. 6G). We did not succeed in detecting EGF-R protein during DMSO-triggered differentiation, although others have described increased EGF-R protein synthesis under similar conditions (45). The Mes-1, End-2, and Epi-7 cell lines showed comparable amounts of EGF-R proteins (Fig. 6E). Thus, whereas the declining IGFI-R levels correlate with increasing amounts of WT1 during differentiation of P19 EC cells, EGF-R levels seem to be unaffected by increased expression of WT1.

Discussion

The work presented here demonstrates that WT1 is differentially regulated in P19 EC cells triggered to differentiate along distinct pathways. Cell types that develop during treatment of P19 EC cells with RA express WT1 (Fig. 2, B and C), whereas WT1 remained undetectable in P19 EC cells differentiated by DMSO (Fig. 2D). Immunohistochemical analysis revealed that subpopulations of WT1-positive, P19-derived cells express either cytokeratin Endo-A (Fig. 3, G and I) or GFAP (Fig. 3, J and L). Thus, endodermal as well as glial cells form in the presence of WT1. Interestingly, cells strongly positive for GFAP and containing long processes are WT1

Fig. 6. Western blot analysis of IGFI-R (*A–D*) and EGF-R (*E–G*) proteins. *A,* IGFI-R is undetectable in P19 cells but present in the Mes-1, End-2, and Epi-7 cell lines. *B,* during differentiation in monolayer, the amount of IGFI-R peaks on day 4 after addition of RA. *C,* IGFI-R proteins increased up to day 5 after replating of RA-treated aggregates before they dropped to undetectable levels at day 8. *D,* during DMSO-triggered differentiation of P19 cells, the amount of IGFI-R increases in time. *E,* EGF-R is absent in P19 cells and expressed in Mes-1, End-2, and Epi-7 cells. *F,* differentiation in monolayer for 6 days (*Lanes 1–6*) leads to a gradual increase of EGF-R protein in time. *G,* EGF-R protein is first detected at day two (*Lane 2*) after replating of P19 aggregates treated with RA and remains virtually constant during 8 days after replating (*Lanes 2–8*). *Thick arrow,* IGFI-R band; *thin arrows,* the EGF-R appears as a doublet of about M_r 155,000 and M_r 165,000.

negative, whereas GFAP and WT1 double-positive cells have a less pronounced phenotype (Fig. 3, J and L). In the embryo, WT1 expression is predominantly found in the urogenital region (46, 47) and also in the nervous system (48, 49). It is tempting to speculate that the WT1 and GFAP double-positive cells are ependymal cells, because ependymal cells express WT1 (49) and are the only glial filament-containing cells that do not form pronounced processes. WT1 may play a common role in the mesenchyme-to-epithelial transition in gonads and kidneys (6), and continuous expression may be necessary for maintenance of the epithelia in these organs. In analogy, we find that the epithelial cell line Epi-7, which originates from RA-induced differentiation of P19 EC cells, contains high levels of WT1 (Fig. 2A), demonstrating that WT1 expression persists in epithelial, P19-derived cells. On the contrary, the mesodermal Mes-1 cell line does not contain WT1 (Fig. 2A).

It is rather unlikely that *WT1* transcription in differentiating P19 EC cells is directly induced by RA, i.e., through a member of the RA-receptor family, because up-regulation is first observed several days after the initiation of RA treatment (Figs. 1A and 2, B and C). Moreover, in HL60 cells differentiated by RA, a down-regulation of *WT1* transcripts is seen (9), and the addition of RA to K562 cells, which do not differentiate in response to RA, does not affect *WT1* mRNA levels (9), indicating that up-regulation of *WT1* is not a direct effect of RA. It has been reported that the decrease of steady-state *WT1* mRNA during differentiation of HL60 and K562 occurs mainly posttranscriptionally (8, 9). Whether the increase of *WT1* transcripts in RA-treated P19 EC cells (Fig. 1A) is primarily caused by enhanced transcription, greater mRNA stability, or a combination of both remains to be investigated. Although several putative transcription factor binding sites have been identified in the promoter of the *WT1* gene (50), only negative autoregulation (51) and the haematopoietic transcription factor GATA-1 (52) have been found to regulate *WT1* expression in vivo. Clearly, additional experiments are needed to unravel the signal-transduction routes that influence WT1 expression, and P19 EC cells may contribute to this end.

It has been reported before that EGR-1 is induced during RA- and DMSO-triggered differentiation of P19 EC cells (44). We now show (Fig. 4) that DNA binding of EGR-1 and WT1 increases during P19 EC cell differentiation, indicating that they can function as transcription factors during differentiation of P19 EC cells. To our knowledge, this is the first report describing the simultaneous induction of WT1 and EGR-1. Intriguingly, DNA binding by EGR-1 increases during P19 EC cell differentiation, regardless of the differentiation pathway, whereas WT1 DNA binding is restricted to RA-triggered differentiation. In P19 EC cells aggregated in the presence of RA, relatively more EGR-1 is present in the DNA binding complex than in P19 EC cells differentiated in monolayer (Fig. 4, B and C). A possible explanation for this is that the cell types that arise during RA treatment as aggregates express higher levels of EGR-1 than those cells arising during RA-triggered differentiation in monolayer. The concomitant increase of WT1 and EGR-1 in P19 EC cells triggered to differentiate by RA may lead to a regulatory system for cer-

tain promoter classes, because EGR-1, which can bind to similar DNA sequences as WT1, in general has opposite effects on transcription regulation (10, 11, 34). Thus, the relative affinities of WT1 and EGR1 for specific promoter elements, together with the ratio between the expression levels of WT1 and EGR1, could be of importance for overall transcription of certain genes during P19 EC cell differentiation.

To date, most reports indicate that WT1 exerts its effects by acting as a repressor of transcription. Interestingly, we found that the amount of IGFI-R protein is inversely correlated with the expression of WT1 in P19 EC cells induced to differentiate by RA (Figs. 2, B and C, and 6, B and C). Furthermore, the steady-state levels of IGFI-R protein are lower in the WT1-positive End-2 and Epi-7 cell lines than in the Mes-1 cell line, which lacks WT1 expression (Figs. 2A and 6A). These results indicate that during RA-induced differentiation of P19 EC cells, WT1 may exert a repressive effect on the IGFI-R promoter, as described (30, 31). These results are consistent with a function for WT1 in repression of IGFI-R transcription. Another putative target for repression by WT1 is the EGF-R promoter (32). However, it had already been found that transcription of the *EGF-R* gene increases 2-fold, and EGF-R protein levels rise about 10-fold during RA-triggered differentiation of P19 EC cells in aggregates (45). Consistently, we found that the amount of EGF-R protein rose to a high level during differentiation of P19 EC cells treated as aggregates with RA on day 2 after replating (Fig. 6G). The increasing amount of EGF-R protein found during RA-triggered differentiation of P19 EC cells in monolayer (Fig. 6F) underscores that the described repressive effect of WT1 on the EGF-R promoter (32) is not found during P19 EC cell differentiation.

The expression of several other putative targets of WT1, including *IGF-II, transforming growth factor β1, platelet-derived growth factor A-chain,* and *EGR-1,* has been characterized in differentiating P19 EC cells (44, 53). However, their expression often is opposite to what would be expected in view of the repressive effect WT1 is reported to have on their promoters (27–29, 34). These discrepancies may be explained in several ways: (a) in transient transfection experiments that are commonly used to study WT1-dependent transcription regulation, a single WT1 form is highly overexpressed, whereas in vivo the four different isoforms are present; and (b) it is now established that the effect of WT1 on transcription regulation in transient transfection assays is dependent on the nature of the expression vector used (54). Furthermore, other transcription factors may mask the effect of WT1 on certain promoters. In this respect, P19 EC cells offer the advantage that *WT1* and *EGR-1* are inducibly expressed from their endogenous promoters, making it possible to test the overall effect that these two transcription factors have on their common target promoters in a more physiological situation. To investigate the effect of WT1 on P19 EC cell differentiation, we have tried extensively to establish P19 EC cells that constitutively overexpress WT1 or the dominant-negative WTAR (55). However, we did not succeed in overexpressing any of the 4 WT1 isoforms or the dominant-negative WTAR. It has been described earlier that

WT1 can induce apoptosis (32). Thus, expression of WT1 in proliferating P19 EC cells may in fact induce apoptosis, which is supported by our preliminary data. As a second approach to address the role of WT1 and EGR-1 in P19 EC differentiation and to identify bona fide target promoters for these two proteins, we are studying the effects of antisense oligonucleotides designed to specifically inhibit WT1 and EGR-1 translation (56, 57) on differentiating P19 EC, End-2, and Epi-7 cells.

In conclusion, we have shown that WT1 expression and DNA binding activity are induced during RA-triggered differentiation of P19 EC cells and that this possibly contributes to the down-regulation of the IGFI-R. Expression of WT1 is detected in epithelial, endodermal, and glial cells. Conversely, DMSO treatment of P19 EC cells fails to induce WT1 expression. Many observations suggest that the *WT1* gene product plays a crucial role during the development of specific embryonic tissues. We believe that the P19 EC cell system might help to elucidate the regulation and functions of WT1 in differentiating cells.

Materials and Methods

Cell Lines and Tissue Culture. The clonal cell lines End-2, Epi-7, and Mes-1 are derived from differentiated P19 cells treated with RA (End-2, Epi-7) and DMSO (Mes-1; Refs. 37 and 38). P19 EC, Mes-1, End-2, and Epi-7 cells were grown on gelatinized Petri dishes in DMEM supplemented with 8% fetal bovine serum in a 5% CO_2 atmosphere. For differentiation in monolayer, the number of cells seeded in medium containing 1 μM all-*trans* RA was adjusted so that the cells had reached approximately 70% confluency on the day of harvesting. For differentiation in aggregates, 2×10^6 cells in 20 ml medium were seeded on bacteriological-grade Petri dishes in media containing either 5×10^{-7} M RA or 1% DMSO. After 3 days, the aggregates were replated on gelatinized tissue culture-grade dishes and cultured for an additional 1 to 8 days in the presence of RA or DMSO. The media were refreshed every other day. 129/Ola-derived ES cells were cultured in DMEM with 10% ES cell-qualified fetal bovine serum on lethally irradiated MEF feeder cells in the presence of 500 units of leukemia inhibitory factor/ml. For differentiation in monolayer, ES cells were seeded on gelatinized tissue culture-grade Petri dishes in leukemia inhibitory factor-deprived medium supplemented with 1 μM RA. The adenovirus-transformed baby rat kidney cell line stably transfected with the human WT1($-/-$) cDNA was described previously (22).

Antibodies. anti-WT1 (C19), EGR1 (588), EGFR (1005), and IGFIRα (N20) antibodies were purchased from Santa Cruz Biotechnology, anti-GFAP antiserum (N1506) was from DAKO, and SSEA-1 and Troma-I (58) were from the Developmental Studies Hybridoma Bank maintained by the John Hopkins University and the University of Iowa.

Immunofluorescence. Cells were grown on gelatinized glass slides in the appropriate medium, washed twice with PBS, and fixed with 80% acetone for 5 min at room temperature. Subsequently, they were rinsed twice with PBS/0.05% Tween 20, preincubated for 1 h with PBS/0.05% Tween 20/5% normal goat serum, incubated for 1 h with the first antibodies and 30 min with the second antibodies coupled to a fluorescent dye (FITC or Rhodamine) diluted in pre-incubation buffer.

Western Blotting. Cells were washed twice with PBS, pelleted, and lysed in ice-cold lysis buffer [50 mM Tris (pH 7.5), 150 mM NaCl, 0.5% NP40, and 10% glycerol supplemented with 1 mM phenylmethylsulfonyl fluoride, 0.1 mg/ml NaF, β-glycero-phosphate, Na_3VO_4, trypsin inhibitor, and 1 mg/ml $Na_4P_2O_7$). After 20 min of incubation on ice, lysates were centrifuged at 4°C for 15 min, and protein concentrations were determined with the Bradford assay (Bio-Rad). Aliquots containing 50 or 100 μg of protein were boiled in sample buffer for 3–5 min before loading onto 10 or 12% SDS-polyacrylamide gels. After blotting onto an Immobilon-P membrane (Millipore), the standard Western procedure was carried out. The first antibodies were diluted 1:500 (WT1) or 1:250 (IGFIRα, EGFR). The second antibody was HRP-conjugated goat antirabbit IgG (Santa Cruz

Biotechnology). Antibody binding was visualized using the Amersham ECL detection system according to the manufacturer's instructions.

Northern Blotting. Total cytoplasmic RNA was extracted from cells with the NP40 method. Twenty μg of each RNA sample were resuspended in RNA loading buffer (50% formamide, 2.2 M formaldehyde, 1× electrophoresis buffer) and electrophoresed through a 1% agarose gel with 2 mM 4-morpholinepropanesulfonic acid, 0.5 mM sodium acetate, and 0.1 mM EDTA as electrophoresis buffer. RNAs were transferred from the gel onto a nitrocellulose membrane (Schleicher & Schuell PH79 membrane filter, 0.1 μm), UV cross-linked for 1 min, and baked for 2 h at 80°C. Membranes were prehybridized at 42°C in prehybridization mix (50% formamide, 5× SSPE, 1% SDS, 5× Denhardt's mix, and 100 μg/ml single-stranded salmon sperm DNA) for over 4 h. DNA fragments were radiolabeled with [α-^{32}P]dATP by the random priming method. Membranes were hybridized overnight at 42°C with prehybridization solution plus the denatured ^{32}P-labeled probe. After hybridization, the blots were washed twice for 15 min at 42°C with 2× SSC/0.1% SDS and exposed to X-ray film with an intensifying screen at -80°C.

Electrophoretic Mobility Shift Assay. Nuclear extracts were prepared by resuspending the cells in 600 μl of swelling buffer [10 mM Tris (pH 7.4), 10 mM NaCl, and 3 mM $MgCl_2$], followed by incubation on ice for 10 min. Next, 35 μl of 10% NP40 were added, and the lysates were vortexed for 10 s before centrifugation for 1 min at 14,000 rpm at 4°C. The pelleted nuclei were resuspended in an equal volume of lysis buffer [20 mM HEPES (pH 7.9), 600 mM KCl, and 0.2 mM EDTA) and left on ice for 30 min with occasional mixing. Subsequently, the lysates were centrifuged at 14,000 rpm for 10 min at 4°C, and the supernatant was resuspended in an equal volume of storage buffer [20 mM HEPES (pH 7.9), 0.2 mM EDTA, and 40% glycerol] and stored at -70°C. All buffers were supplemented with 1 mM phenylmethylsulfonyl fluoride, 0.1 mg/ml NaF, 0.1 mg/ml β-glycero-phosphate, 0.1 mg/ml Na_3VO_4, 0.1 mg/ml trypsin inhibitor, 1 mg/ml $Na_4P_2O_7$, and 1 mM DTT.

A pair of 21-bp synthetic oligonucleotides containing the WTE DNA sequence 5'-AATTCTACTCCCCACGCACTCG-3' (23) was used as probe for the assay. The probe was labeled by filling in the cohesive ends of 5 pM of the fragment with [α-^{32}P]dATP and [α-^{32}P]dCTP before the final volume was adjusted to 100 μl. Nuclear extract (2.5 or 5 μg; P19 differentiated as aggregates in the presence of RA or DMSO) was used in each binding reaction. Where appropriate, the extract was preincubated for 10 min at room temperature with either 0.1 μg of EGR1/WT1 antibody, 5 pM of unlabeled WTE oligo, or 5 pM of unspecific competitor. Subsequently, binding to 1 μl of radioactive WTE oligo was carried out in a reaction mixture containing 1 μg of poly(dI-dC), 20 mM HEPES (pH 7.6), 70 mM KCl, 5 mM $MgCl_2$, 0.05% NP40, 12% glycerol, 1 mg/ml BSA, 0.5 mM DTT, and 0.1 mM $ZnCl_2$ for 30 min at room temperature. DNA-protein complexes were separated on a 4% nondenaturing PAA gel and visualized by autoradiography.

Acknowledgments

References

1. Beckwith, J. B., Kiviat, N. B., and Bonadio, J. F. Nephrogenic rests, nephroblastomatosis, and the pathogenesis of Wilms' tumor. Pediatr. Pathol., *10:* 1–36, 1990.

2. Reddy, J. C., and Licht J. D. The *WT1* Wilms' tumor suppressor gene: how much do we really know? Biochim. Biophys. Acta, *1287:* 1–28, 1996.

3. Pritchard-Jones, K., Flemming, S., Davidson, D., Bickmore, W., Porteous, D., Gosden, C., Bard, J., Buckler, A., Pelletier, J., Housman, D., van Heyningen, V., and Hastie, N. The candidate Wilms' tumor gene is involved in genitourinary development. Nature (Lond.), *346:* 194–197, 1990.

4. Buckler, A. J., Pelletier, J., Haber, D. A., Glaser, T., and Housman, D. E. Isolation, characterization, and expression of the murine Wilms' tumor gene (*WT1*) during kidney development. Mol. Cell. Biol., *11:* 1707–1712, 1991.

5. Coppers, M. J., Campbell, C. E., and Williams, B. R. G. The role of *WT1* in tumorigenesis. FASEB J., *7:* 886–895, 1993.

6. Hastie, N. D. The genetics of Wilms' tumor—a case of disrupted development. Annu. Rev. Genet., *28:* 523–558, 1994.

7. Kreidberg, J. A., Hannu, S., Loring, J. M., Maedra, M., Pelletier, J., Housman, D., and Jaenisch, R. WT-1 is required for early kidney development. Cell, *74:* 679–691, 1993.

8. Phelan, S. A., Lindberg, C., and Call, K. M. Wilms' tumor gene, *WT1,* mRNA is downregulated during induction of erythroid and megakaryocytic differentiation ofK562 cells. Cell Growth & Differ., *5:* 677–686, 1994.

9. Sekiya, M., Adachi, M., Hinoda, Y., Imai, K., and Yachi, A. Downregulation of Wilms' tumor gene (*wt1*) during myelomonocytic differentiation in HL60 cells. Blood, *83:* 1876–1882, 1994.

10. Kinane, T. B., Finder, J. D., Kawashima, A., Brown, D., Abbate, M., Shang, C., Fredericks, W. J., Rauscher, F. J., Sukhatme, V. P., and Ercolani, L. Growth of LLC-PK1 renal cells is mediated by EGR-1 up-regulation of G protein $_{\alpha i-2}$ protooncogene transcription. J. Biol. Chem., *269:* 27503–27509, 1994.

11. Kinane, T. B., Finder, J. D., Kawashima, A., Brown, D., Abbate, M., Fredericks, W. J., Sukhatme, V. P., Rauscher, F. J., III, and Ercolani, L. LLC-PK$_1$ cell growth is repressed by WT1 inhibition of G-protein$_{\alpha i-2}$ protooncogene transcription. J. Biol. Chem., *271:* 30760–30764, 1996.

12. McBurney, M. W., and Rogers, B. J. Isolation of male murine embryonal carcinoma cells and their chromosome replication patterns. Dev. Biol., *89:* 503–508, 1982.

13. Evans, M. J., and Kaufmann, M. H. Establishment in culture of pluripotential cells from mouse embryos. Nature (Lond.), *292:* 154–156, 1981.

14. Martin, G. A. Isolation of a pluripotent cell line from early mouse embryos cultured in medium conditioned by teratocarcinoma stem cells. Proc. Natl. Acad. Sci. USA, *78:* 7634–7638, 1981.

15. Doetschmann, T. C., Eistetter, H., Katz, M., Schmidt, W., and Kemler, R. The *in vitro* development of blastocyst-derived embryonic stem cell lines: formation of visceral yolk sac, blood islands and myocardium. J. Embryol. Exp. Morphol., *87:* 27–45, 1985.

16. McBurney, M. W. P19 embryonal carcinoma cells. Int. J. Dev. Biol., *37:* 135–140, 1993.

17. Jones-Villeneuve, E. M. V., McBurney, M. W., Rogers, A., and Kalnins, V. I. Retinoic acid induces embryonal carcinoma cells to differentiate into neurons and glial cells. J. Cell Biol., *94:* 253–262, 1982.

18. McBurney, M. W., Reuhl, K. R., Ally, A. I., Nasipuri, S., Bell, J. C., and Craig, J. Differentiation and maturation of embryonal carcinoma-derived neurons in cell culture. J. Neurosci., *8:* 1063–1073, 1988.

19. van der Kruijssen, C. M. M., van Achterberg, T. A. E., Hébert, J. M., de Waele, P., and van den Eijnden-van Raaij, A. J. M. Neuronal and meso-dermal differentiation of P19 embryonal carcinoma cells is characterized by expression of specific marker genes and modulated by activin and fibroblast growth factors. Dev. Growth Differ., *37:* 559–574, 1995.

20. McBurney, M. W., Jones-Villeneuve, E. M. V., Edwards, M. K. S., and Anderson, P. J. Control of muscle cell and neuronal differentiation in a cultured embryonal carcinoma cell line. Nature (Lond.), *299:* 165–167, 1982.

21. Edwards, M. K. S., Harris, J. F., and McBurney, M. W. Induced muscle cell differentiation in an embryonal carcinoma cell line. Mol. Cell. Biol., *3:* 2280–2286, 1983.

22. Mummery, C. L., Feijen, A., van der Saag, P. T., van den Brink, C. E., and de Laat, S. W. Clonal variants of differentiated P19 embryonal carcinoma cells exhibit epidermal growth factor receptor kinase activity. Dev. Biol., *109:* 402–410, 1985.

23. Mummery, C. L., Feijen, A., Moolenaar, W. H., van den Brink, C. E., and de Laat, S. W. Establishment of a differentiated mesodermal line from P19 EC cells expressing functional PDGF and EGF receptors. Exp. Cell Res., *165:* 229–242, 1986.

24. Gashler, A., and Sukhatme, V. P. Early growth response protein 1 (EGR-1): prototype of a zinc-finger family of transcription factors. Prog. Nucleic Acid Res. Mol. Biol., *50:* 191–224, 1995.

25. Haber, D. A., Sohn, R. L., Buckler, A. J., Pelletier, J., Call, K. M., and Housman, D. E. Alternative splicing and genomic structure of the Wilms' tumor gene *WT1.* Proc. Natl. Acad. Sci. USA, *88:* 9618–9622, 1991.

26. Morris, J. F., Madden, S. L., Tournay, A. E., Cook, D. M., Sukhatme, V. P., and Rauscher, F. J., III. Characterization of the zinc finger protein encoded by the Wilms' tumor locus. Oncogene, *6:* 2339–2348, 1991.

27. Gashler, A. L., Bonthron, D. T., Madden, S. L., Rauscher, F. J., III, Collins, T., and Sukhatme, V. P. Human platelet-derived growth factor A chain is transcriptionally repressed by the Wilms tumor suppressor WT1. Proc. Natl. Acad. Sci. USA, *89:* 10984–10988, 1992.

28. Drummond, I. A., Madden, S. L., Rohwer-Nutter, P., Bell, G. I., and Rauscher, F. J., III. Repression of the insulin-like growth factor II gene by the Wilms tumor suppressor WT1. Science (Washington DC), *257:* 674–678, 1992.

29. Dey, B. R., Sukhatme, V. P., Roberts, A. B., Sporn, M. B., Rauscher, F. J., III, and Kim, S-J. Repression of the transforming growth factor-β1 gene by the Wilms' tumor suppressor *WT1* gene product. Mol. Endocrinol., *8:* 595–602, 1994.

30. Werner, H., Re, G. G., Drummond, I. A., Sukhatme, V. P., Rauscher, F. J., III, Sens, D. A., Garvin, A. J., LeRoith, D., and Roberts, C. T., Jr. Increased expression of the insulin-like growth factor I receptor gene, *IGFIR,* in Wilms' tumor is correlated with modulation of *IGFIR* promoter activity by the *WT1* Wilms' tumor gene product. Proc. Natl. Acad. Sci. USA, *90:* 5828–5832, 1993.

31. Werner, H., Shen-Orr, Z., Rauscher, F. J., III, Morris, J. F., Roberts, C. T., Jr., and LeRoith, D. Inhibition of cellular proliferation by the Wilms tumor suppressor WT1 is associated with suppression of insulin-like growth factor I receptor gene expression. Mol. Cell. Biol., *15:* 3516–3522, 1995.

32. Englert, C., Hou, X., Kaheswaran, S., Bennett, P., Ngwu, C., Re, G. G., Garvin, A. J., Rosner, M. R., and Haber, D. A. WT1 suppresses synthesis of the epidermal growth factor receptor and induces apoptosis. EMBO J., *14:* 4662–4675, 1995.

33. Ryan, G., Steele-Perkins, V., Morris, J. F., Rauscher, F. J., III, and Dressler, G. R. Repression of *Pax-2* by *WT1* during normal kidney development. Development (Camb.), *121:* 867–875, 1995.

34. Madden, S. L., Cook, D. M., Morris, J. F., Gashler, A., Sukhatme, V. P., and Rauscher, F. J., III. Transcriptional repression mediated by the *WT1* Wilms' tumor gene product. Science (Washington DC), *253:* 1550–1553, 1991.

35. Larsson, S. H., Charlieu, J. P., Miyagawa, K., Engelkamp, D., Rassoulzadegan, M., Ross, A., Cuzin, F., van Heyningen, V., and Hastie, N. D. Subnuclear localization of WT1 in splicing and transcription factor domains is regulated by alternative splicing. Cell, *81:* 391–401, 1995.

36. Kennedy, D., Ramsdale, T., Mattick, J., and Little, M. An RNA recognition motif in Wilms' tumor protein (WT1) revealed by structural modelling. Nat. Genet., *12:* 329–332, 1996.

37. Rauscher, F. J., III, Morris, J. F., Tournay, O. E., Cook, D. M., and Curran, T. Binding of the Wilms' tumor locus zinc finger protein to the EGR-1 consensus sequence. Science (Washington DC), *250:* 1259–1262, 1990.

38. Menke, A. L., Riteco, N., van Ham, R. C. A., de Bruyne, C., Rauscher, F. J., III, van der Eb, A. J., and Jochemsen, A. G. Wilms' tumor 1 splice variants have opposite effects on the tumorigenicity of adenovirus-trans-formed baby rat kidney cells. Oncogene, *12:* 537–546, 1996.

39. Nakagama, H., Heinrich, G., Pelletier, J., and Housman, D. E. Sequence and structural requirements for high-affinity DNA binding by the *WT1* gene product. Mol. Cell. Biol., *15:* 1489–1498, 1995.

40. Mummery, C. L., Feyen, A., Freund, E., and Shen, S. Characteristics of embryonic stem cell differentiation: a comparison with two embryonal carcinoma cell lines. Cell Differ. Dev., *30:* 195–206, 1990.

41. Bruening, W., and Pelletier, J. A non AUG translational initiation event generates novel WT1 isoforms. J. Biol. Chem., *271:* 8646–8654, 1996.

42. Solter, D., and Knowles, B. B. Monoclonal antibody defining a stage-specific mouse embryonic antigen (SSEA-1). Proc. Natl. Acad. Sci. USA, *75:* 5565–5569, 1978.

43. Mundlos, S., Pelletier, J., Darveau, A., Bachmann, M., Winterpacht A., and Zabel, B. Nuclear localization of the protein encoded by the Wilms' tumor gene *WT1* in embryonic and adult tissues. Development (Camb.), *119:* 1329–1341, 1993.

44. Darland, T., Samuels, M., Edwards, S. A., Sukhatme, V. P., and Adamson, E. D. Regulation of EGR-1 (Zfp-6) and c-*fos* expression in differentiating embryonal carcinoma cells. Oncogene, *6:* 1367–1376, 1991.

45. Joh, T., Darland, T., Samuels, M., Wu, J-X., and Adamson, E. D. Regulation of epidermal growth factor receptor gene expression in embryonal carcinoma cells. Cell Growth & Differ., *3:* 315–325, 1992.

46. Armstrong, J. F., Pritchard-Jones, K., Bickmore, W. A., Hastie, N. D., and Bard, J. B. L. The expression of the Wilms' tumor gene, *WT1,* in the developing mammalian embryo. Mech. Dev., *40:* 85–97, 1992.

47. Kent, J., Corriat, A-M., Sharpe, P. T., Hastie, N. D., and van Heyningen, V. The evolution of WT1 sequence and expression pattern in the vertebrates. Oncogene, *11:* 1781–1792, 1995.

48. Sharma, M. P., Yang, X., Bowman, M., Roberts, V., and Sukumar, S. Molecular cloning of rat Wilms' tumor complementary DNA and a study of messenger RNA expression in the urogenital system and the brain. Cancer Res., *52:* 6407–6412, 1992.

49. Rackley, R. R., Flenniken, A. M., Kuriyan, N. P., Kessler, P. M., Stoler, M. H., and Williams, B. R. G. Expression of the Wilms' tumor suppressor gene *WT1* during mouse embryogenesis. Cell Growth & Differ., *4:* 1023–1031, 1993.

50. Fraizer, G. C., Wu, Y-J., Hewitt, S. M., Maity, T., Ton, C. C. T., Huff, V., and Saunders, G. F. Transcriptional regulation of the human Wilms' tumor gene (*WT1*). J. Biol. Chem., *269:* 8892–8900, 1994.

51. Rupprecht, H. D., Drummond, I. A., Madden, S. L., Rauscher, F. J., III, and Sukhatme, V. P. The Wilms' tumor suppressor gene *WT1* is negatively autoregulated. J. Biol. Chem., *269:* 6198–6206, 1994.

52. Wu, Y-J., Fraizer, G. C., and Saunders, G. F. GATA-1 transactivates the WT1 hematopoietic specific enhancer. J. Biol. Chem., *270:* 5944–5949, 1995.

53. Mummery, C. L., van den Eijnden-van Raaij, A. J. M., Feijen, A., Freund, E., Hulskotte, E., Schoorlemmer, J., and Kruijer, W. Expression of growth factors during the differentiation of embryonic stem cells in monolayer. Dev. Biol., *142:* 406–413, 1990.

54. Reddy, J. C., Hosono, S., and Licht, J. D. The transcriptional effect of WT1 is modulated by choice of expression vector. J. Biol. Chem., *270:* 29976–29982, 1995.

55. Haber, D. A., Timmers, H. T. M., Pelletier, J., Sharp, P. A., and Housman, D. E. A dominant mutation in the Wilms tumor gene *WT1* cooperates with the viral oncogene *E1A* in the transformation of primary kidney cells. Proc. Natl. Acad. Sci. USA, *89:* 6010–6014, 1992.

56. Algar, E. M., Khromykh, T., Smit, S. I., Blackburn, D. M., Bryson, G. J., and Smith, P. J. A WT1 antisense oligonucleotide inhibits proliferation and induces apoptosis in myeloid leukemia cell lines. Oncogene, *12:* 1005–1014, 1996.

57. Muthukkumar, S., Nair, P., Sells, S. F., Maddiwar, N. G., Jacob, R. J., and Rangnekar, V. M. Role of EGR-1 in thapsigargin-inducible apoptosis in the melanoma cell line A375-C6. Mol. Cell. Biol., *15:* 6262–6272, 1995.

58. Brulet, P., Babinet, C., Kemler, R., and Jacob, F. Monoclonal antibodies against trophectoderm-specific markers during mouse blastocyst formation. Proc. Natl. Acad. Sci. USA, *77:* 4113–4117, 1980.